Catalysis Today 146 (2009) 20–24

Contents lists available at ScienceDirect

Catalysis Today

journal homepage: www.elsevier.com/locate/cattod

PtRu overlayers on Au nanoparticles for methanol electro-oxidation

Kug-Seung Lee, In-Su Park, Hee-Young Park, Tae-Yeol Jeon, Yung-Eun Sung *

School of Chemical & Biological Engineering and Research Center for Energy Conversion & Storage, Seoul National University, Seoul 151-744, South Korea

ARTICLE INFO

Article history:
Available online 31 March 2009

Keywords:
Direct methanol fuel cell
Overlayer structure
PtRu-modified Au nanoparticles
Methanol electro-oxidation

ABSTRACT

PtRu overlayer structures were deposited on the surface of carbon-supported Au nanoparticles with atomic-scale thicknesses and their activity for methanol electro-oxidation was examined. The results of transmission electron microscopy, X-ray diffraction, and cyclic voltammetry demonstrated that the PtRu deposited uniformly on Au nanoparticles. The peak potential in CO stripping analysis shifted to higher potentials with decreasing amounts of PtRu, indicating stronger Pt–CO and Ru–CO bonding. PtRu utilization was enhanced with decreasing PtRu, which might be attributed to the overlayer structures on Au substrates. In methanol electro-oxidation, a negative effect of the strengthened Pt–CO and Ru–CO bonding on surface specific activity and a positive effect of PtRu utilization on mass specific activity might contribute competitively to overall activity for methanol electro-oxidation.

1. Introduction

Direct methanol fuel cells (DMFCs) have been considered ideal power sources for potable electronic devices. A great deal of research on methanol electro-oxidation has been conducted so far on finding optimal materials for the catalyst, on effective surface structures, and on lowering the overall cost of DMFCs. However, DMFCs are still limited by high production costs due to heavy loading of Pt and its alloy materials. One major effort, nowadays, is on enhancing Pt utilization through modifying the surfaces of non-Pt nanoparticles [1–3]. The Pt utilization in catalysts can be defined as the dispersion or exposed percentage of Pt atoms in the catalyst [1].

Recently, we reported electrocatalytic activities of Pt-modified Au nanoparticles using a successive reduction process [3,4]. Pt-modified Au nanoparticles were synthesized using a highly dispersed Au substrate, resulting in high Pt utilization and greatly enhanced mass specific activities in methanol electro-oxidation. In addition to the high Pt utilization, it was reported, by Zhao and Xu [1], that Pt-modified Au nanoparticles showed high stability in methanol electro-oxidation. However, Pt cannot be used alone in real DMFC catalysts because CO species can be adsorbed on Pt surface during methanol electro-oxidation and can block further adsorption of methanol.

Pt-based bimetallic catalysts (including PtRu, PtSn, PtW, and PtOs) have been investigated, and PtRu electrode has shown the most promising results among them. The role of second metals in the catalysts has been known to be the supplying of OH species at low potentials and/or the weakening of the Pt–CO bond [5,6]. Therefore, it is desirable to modify Au nanoparticles with PtRu bimetallic overlayers.

In surface-modified catalysts, the intrinsic activities of active sites, in addition to the Pt utilization, are also worthy of consideration for the interaction between underlayer and overlayer materials (between Au and PtRu in this case). It is interesting that the Pt–CO bond on Pt-modified Au substrate becomes weaker or stronger than that on the surface with Pt alone. Zeng et al. [7] reported that the CO stripping peak of core-shell Au-Pt nanoparticles was located at potential more negative than that of Pt/C while Du and Tong [8] reported opposite results. In our previous publication [9], Pt-modified Au nanoparticles showed higher mass specific activity but lower area specific activity than Pt/C. We explained that the results can be attributed to (1) the strengthened Pt–CO bonding or the weakened ensemble effect and (2) the enhanced Pt utilization.

In this work, PtRu bimetallic species were deposited onto carbon-supported Au nanoparticles (Au/C) with atomic-scale thicknesses and were applied as catalysts for methanol electro-oxidation. Various amounts of PtRu were loaded onto Au nanoparticles and their surface structures and electrocatalytic activities were investigated.

2. Experimental

2.1. Catalyst preparation

All aqueous solutions were prepared with deionized (DI) water, which was further purified with a Milli-Q system (Millipore water,

* Corresponding author. Tel.: +82 2 8801889; fax: +82 2 8881604.
E-mail address: ysung@snu.ac.kr (Y.-E. Sung).

0920-5861/$ – see front matter © 2009 Elsevier B.V. All rights reserved.
doi:10.1016/j.cattod.2009.02.031

18.2 MΩ cm). The following chemicals were obtained from Aldrich: $HAuCl_4{\cdot}3H_2O$, $H_2PtCl_6{\cdot}xH_2O$, sodium citrate tribasic dihydrate ($Na_3C_6H_5O_7{\cdot}2H_2O$), $NaBH_4$, and ethylene glycol (EG). All chemicals were of analytical grade and were used as received.

The details for preparing Au/C were presented in our previous reports [3,4]. The 30 wt% Au/C was prepared as follows: Au colloid nanoparticles were prepared by adding $HAuCl_4{\cdot}3H_2O$ to DI water, followed by the addition of aqueous sodium citrate. Then, $NaBH_4$ and sodium citrate dissolved solution were added quickly with vigorous stirring [10]. The solution was stirred for 30 min, and then carbon black (Vulcan XC-72R) was added. Au colloid particles were supported spontaneously on the surface of the carbon black particles during the 48 h stirring period. Finally, the solution was filtered and evaporated.

The PtRu overlayers on Au nanoparticles were prepared using a polyol reduction process and the procedure is as follows: Pt precursor ($H_2PtCl_6{\cdot}xH_2O$) and Ru precursor ($RuCl_3{\cdot}xH_2O$) were dissolved in EG and adequate amounts of the solutions were added to Au/C-dispersed EG solution. The total volume of the solution was 200 ml. The solution was refluxed in a three-neck flask at 80 °C for 12 h. After cooling at room temperature, the solution was filtered, washed with DI water and ethanol, and then evaporated. The amounts of Pt and Ru precursors were calculated to produce an atomic ratio of Pt:Ru = 2:1. The PtRu:Au ratio was adjusted to create samples with PtRu:Au atomic ratios of 0.25:1, 0.5:1, 0.75:1 and 1:1. Hereafter, the PtRu overlayers on Au/C samples are designated as SPR-[x] (x = the PtRu/Au atomic ratio). For comparison, 60 wt% Pt_2Ru_1/C was synthesized in EG at 160 °C for 3 h, which is designated as PtRu/C.

2.2. Catalyst characterization

High resolution-transmission electron micrographs (HR-TEM) were obtained on a JEOL 2010 operated at 200 kV. Samples were prepared by placing a drop of catalyst solution onto a carbon-coated copper grid and then drying. Analysis of X-ray diffraction (XRD) was performed using a Rigaku D/MAX 2500 operated with a Cu Kα source (λ = 1.541 Å) at 40 kV and 200 mA. The samples were scanned from 30° to 55° (2θ) with a scan rate of 2°/min. X-ray photoelectron spectroscopy (XPS) was performed using an ESCALAB 220I XL (Thermo Electron) photoelectron spectrometer. The X-ray source was Al Kα operating at 10 kV and 120 W. Samples were prepared by depositing the catalysts on an Si wafer using double-sided tape. Energy dispersive X-ray (EDX) analysis was carried out using an SEM-EDX system (JEOL, JSM-7000F).

Cyclic voltammogram was obtained in a conventional three-electrode electrochemical cell using a glassy carbon (GC) electrode (6 mm diameter) as a working electrode, and Pt wire and saturated calomel electrode as a counter and a reference electrode, respectively [11–16]. Electrochemical measurements were all recorded and reported vs. normal hydrogen electrode (NHE). The GC electrode was polished with 1, 0.3, 0.05 μm-Al_2O_3 slurry and washed ultrasonically with DI water before use. The ink slurry was prepared by mixing carbon-supported nanoparticles, a 5 wt%

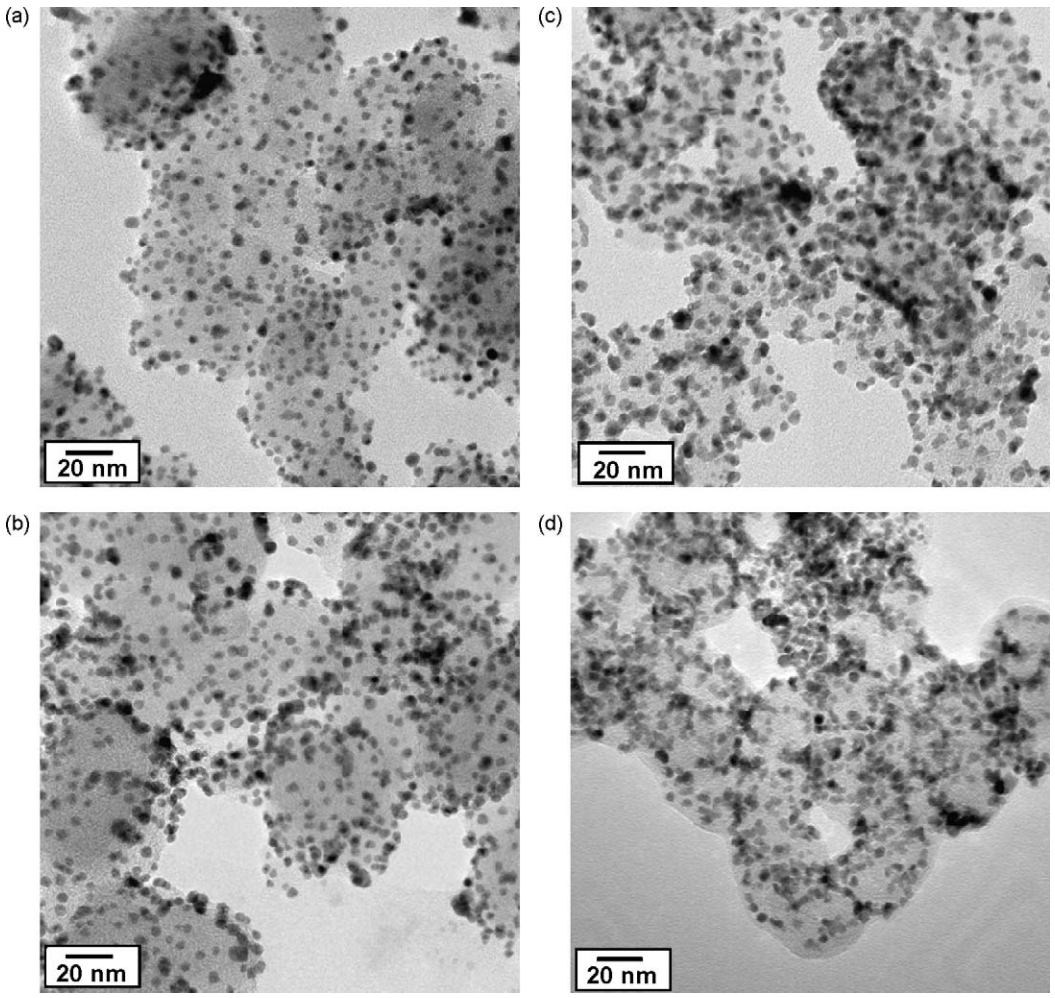

Fig. 1. TEM images of the Au and PtRu overlayers on Au nanoparticles: (a) Au/C, (b) SPR-[0.5], (c) SPR-[1], and (d) PtRu/C.

Nafion® solution (Aldrich Chem. Co), and 2-propanol. The ratio of components in the catalyst ink was 60 μl of DI water, 600 μl of Nafion® solution and 6 ml of 2-propanol per 0.1 g of catalysts. The catalyst ink was dropped onto a glassy carbon electrode using a micropipette, and then dried in a vacuum oven. Electrochemical experiments were performed with an Autolab general purpose electrochemical system (Eco Chemie). Solutions of 0.5 M H_2SO_4 and 1 M CH_3OH + 0.5 M H_2SO_4 were purged with Ar gas prior to taking measurements. In order to identify the activities of the electrocatalysts, cyclic voltammetry (CV) was conducted at potentials between 0.05 and 1 V vs. NHE at a scan rate of 20 mV/s. CO stripping voltammetry was performed at potentials between 0.05 and 1.2 V vs. NHE at a scan rate of 50 mV/s. CO molecules were attached to catalysts at a potential of 0.1 V vs. NHE by bubbling a 0.5 M H_2SO_4 solution with 10% CO/He gas for 20 min and then the dissolved CO gas in the solution was removed by bubbling with Ar gas for 30 min. All electrochemical experiments were performed at room temperature.

3. Results and discussion

3.1. Structural characterizations

The Au and PtRu overlayers on Au nanoparticles were well-dispersed on carbon support as shown Fig. 1. Mean diameters from TEM for Au, SPR-[0.5], SPR-[1], and PtRu/C were 3.89, 4.36, 4.75, and 4.45 nm, respectively. Theoretical diameters of SPR catalysts were calculated using the following equation [1]:

$$D_{\mathrm{PtRu-Au}} = D_{\mathrm{Au}}\left(1 + [\mathrm{PtRu}]\frac{V_m(\mathrm{Pt})\rho_{\mathrm{Pt}} + V_m(\mathrm{Ru})\rho_{\mathrm{Ru}}}{V_m(\mathrm{Au})[\mathrm{Au}]}\right)^{1/3}$$

where V_m is the molar volume, [ ] the atomic ratio between PtRu and Au (here [PtRu]/[Au] = 0.5 for SPR-[0.5], 1 for SPR-[1]), $D_{\mathrm{PtRu-Au}}$ the diameter of the Pt_xRu_y–Au nanoparticles, D_{Au} the diameter of the carbon-supported Au nanoparticles, and ρ the atomic fraction between Pt and Ru (ρ_{Pt} = 0.67 and ρ_{Ru} = 0.33). The calculated mean diameters were 4.38 nm for SPR-[0.5] and 4.79 nm SPR-[1], which were corresponded closely to the experimental values. The diameters of SPR-[0.5] and SPR-[1] suggest 0.25 and 0.45 nm thicknesses of the PtRu overlayer and thus ~0.9 and ~1.7 monolayer for SPR-[0.5] and SPR-[1], respectively (d_{Pt} = 0.276 and d_{Ru} = 0.268 nm) [17].

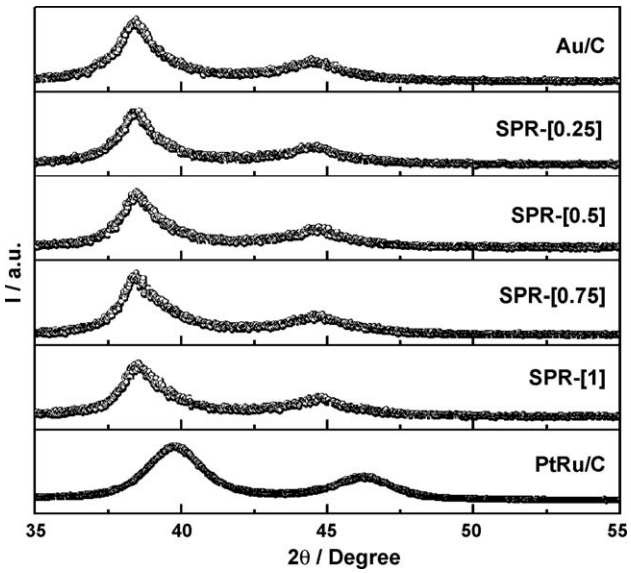

Fig. 2. XRD profiles of the prepared samples.

Table 1
Bulk and surface compositions of the catalysts from EDX and XPS, respectively. Values in parentheses are surface compositions.

Element	SPR-[1]	SPR-[0.5]	SPR-[0.25]	PtRu/C
Pt	33.5 (45.6)%	22.5 (34.4)%	16.3 (26.0)%	64.7 (58.2)%
Ru	16.7 (21.9)%	11.1 (18.3)%	7.8 (12.9)%	35.3 (41.8)%
Au	49.8 (32.5)%	66.4 (47.3)%	75.9 (61.1)%	–

Fig. 2 shows XRD profiles of the prepared samples. The Au/C exhibited typical polycrystalline Au diffraction (38.3° for Au (1 1 1) and 44.5° for Au (2 0 0)). The peak positions of the PtRu overlayers on Au/C keep their initial positions, implying that Au and PtRu did not form alloy structures although a small possibility for forming surface alloy cannot be ignored. Pt, Ru, and/or PtRu alloy diffraction peaks were not detected, possibly because they were deposited too thinly onto the Au substrate to be detected. Instead, the diffraction profile of Au (1 1 1) is distorted as the loaded amount of PtRu increased. This might be due to the modified structure of PtRu overlayer on Au nanoparticles [3]. The detailed structures of the PtRu overlayers on Au nanoparticles should be investigated further.

Bulk and surface compositions of the catalysts were measured by EDX and XPS, respectively. As shown in Table 1, the result of EDX corresponds to the nominal values. XPS result shows slightly different compositions from that of EDX due to the difference in bulk and surface compositions. Both in EDX and XPS results for SPR catalysts, Pt/Ru ratios of SPR catalysts are nearly 2. These results

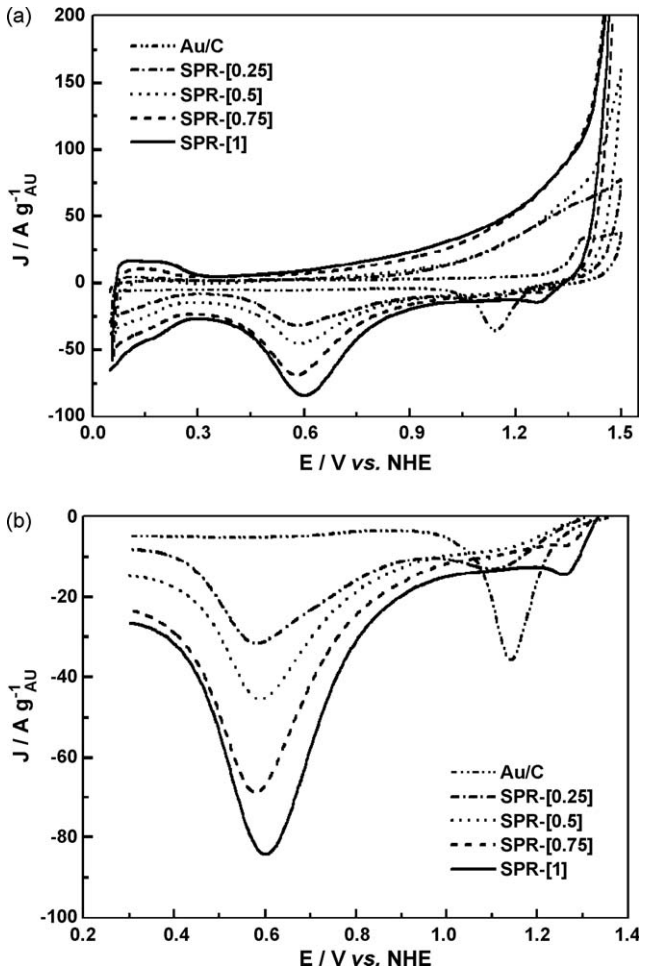

Fig. 3. Cyclic voltammetric analysis of (a) the Au and PtRu overlayers on Au nanoparticles in 0.5 M H_2SO_4 and (b) magnified one of negative-going scans.

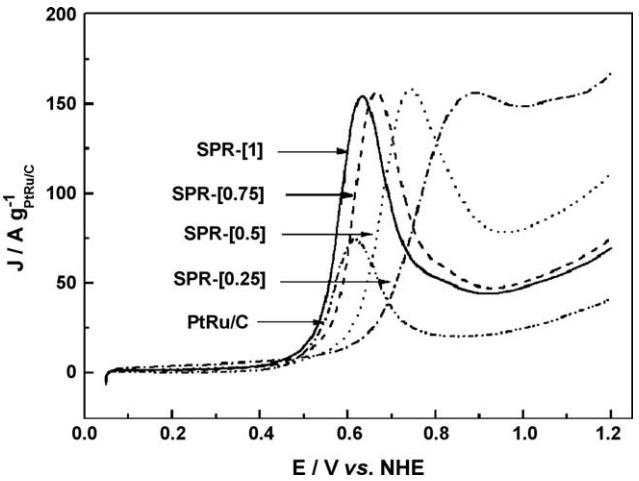

Fig. 4. Positive-going scans from CO stripping analysis in 0.5 M H_2SO_4.

indicate all of the metal salts were reduced during the synthesis. The surface composition of PtRu/C shows higher Ru content than the bulk composition due to the different reduction rates of Pt and Ru salts.

3.2. Surface characterizations

Surface characteristics of the prepared samples were investigated using cyclic voltammetry in 0.5 M H_2SO_4 and are shown in Fig. 3. The currents were normalized by Au mass. The PtRu overlayers on Au nanoparticles showed well-defined profiles in the hydrogen and oxygen adsorption–desorption regions. As the loaded amount of PtRu increased, the hydrogen and oxygen adsorption–desorption area increased. The high anodic current at the potentials higher than 1.4 V can be attributed to oxygen evolution, oxide formation, and dissolution of the overlayers [18,19]. The negative-going scans are magnified in Fig. 3(b). As the PtRu amount decreases, the Ru oxide reduction peak at 1.25 V [20] becomes negligible, indicating that most elemental Ru dissolved during high anodic potential scan. Also, the Au oxide reduction peak at 1.1–1.2 V becomes prominent, indicating that Au surface exposed significantly because the PtRu amount was not enough to cover all Au sites. The Au oxide reduction peaks for SPR-[0.75] and SPR-[1] were hardly detectable, which means that all Au sites were covered by PtRu overlayer. Based on the results of TEM, XRD, and cyclic voltammetry, it is demonstrated that the carbon-supported Au nanoparticles were modified with PtRu to form PtRu overlayer structures at atomic-scale thicknesses.

CO stripping analysis was carried out in 0.5 M H_2SO_4 and the results normalized by PtRu mass are shown in Fig. 4. The CO stripping peak positions, onset potentials, and electrochemical surface areas (normalized by PtRu mass) calculated using CO stripping area are listed in Table 2. The peak positions and onset potentials of the PtRu overlayers on Au nanoparticles were higher than that of PtRu/C and shifted positively with decreasing PtRu amount. This result indicates that Pt–CO and Ru–CO bonding of PtRu overlayers on Au nanoparticles is stronger than that of PtRu/C

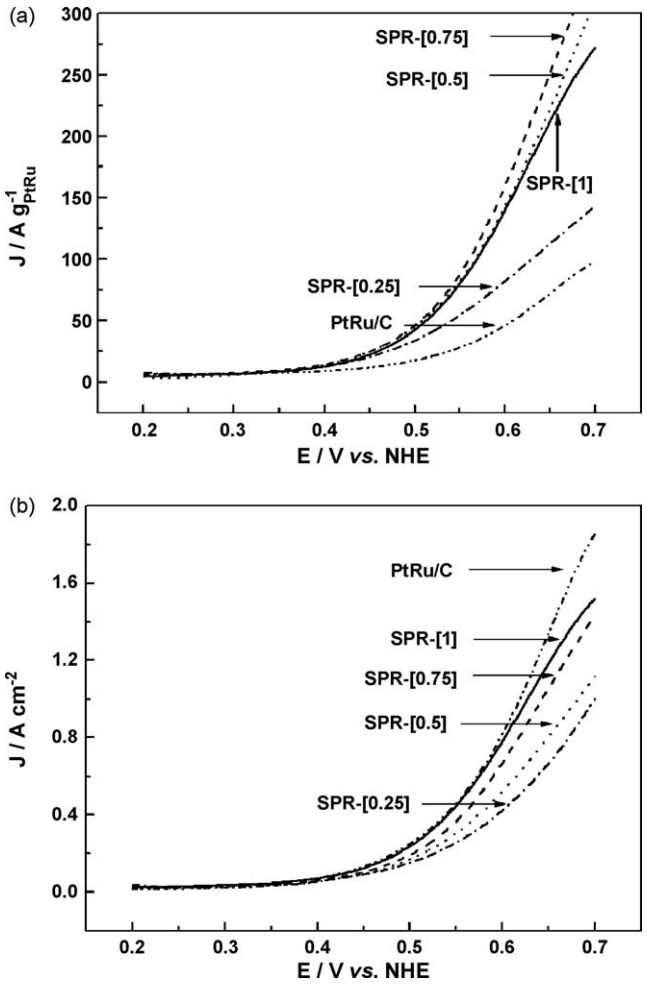

Fig. 5. (a) Mass specific and (b) surface specific current densities for methanol electro-oxidation in 0.5 M H_2SO_4 + 1 M MeOH.

[8,20]. In the report by Du and Tong, the positive shift in peak potentials of CO stripping with increasing Pt coverage on Au substrate was observed and was attributed to stronger Pt–CO bonding. Two peaks were observed in the study: one was associated with narrow CO stripping peaks and active for MeOH electro-oxidation, and the other was associated with broad CO stripping peaks and inactive for MeOH electro-oxidation. They assigned the narrow and broad CO stripping peaks to large and small (dispersed Pt adatoms) Pt islands, respectively. In the present experiment, the CO stripping peaks were not divided into two peaks, but only single peaks were observed and the peaks were broadened with decreasing PtRu amount. Although the peak number of CO stripping is not the same as Du and Tong's study, the peak shift and broadening with decreasing PtRu amount can be attributed to strengthened Pt–CO and Ru–CO bonding. In the report by Štrbac et al., Ru on Au also showed positive shift in CO stripping peak. These stronger Pt–CO and Ru–CO bonding on Au substrate were predicted by Hammer–Norskov d-band center

Table 2
Summary of CO stripping analysis.

	Sample				
	SPR-[1]	SPR-[0.75]	SPR-[0.5]	SPR-[0.25]	PtRu/C
Electrochemical surface area (cm^2/g_{PtRu})	101.3	105.4	118.4	123.3	61.7
Onset potential (V vs. NHE)	0.39	0.41	0.45	0.52	0.36
Peak potential (V vs. NHE)	0.634	0.665	0.743	0.892	0.615

model [21]. In the d-band center model, Pt and Ru d-band centers can be up shifted on Au, and this can be related to the strengthened Pt–CO and Ru–CO bonding. The electrochemical surface area of the PtRu overlayers on Au nanoparticles was higher up to 200% than that of PtRu/C and increased with decreasing PtRu amount, indicating higher PtRu utilization and uniformly deposited PtRu overlayers.

3.3. Methanol electro-oxidation

The electrocatalytic activities of PtRu overlayers on Au nanoparticles were measured by obtaining a voltammogram in a solution of 0.5 M H_2SO_4 + 1 M CH_3OH. The oxidation current was normalized by PtRu mass and is given in the range of 0.2–0.7 V for clarity. As shown in Fig. 5(a), the activity order at low potentials (less than 0.6 V) is as follows: SPR-[0.75], SPR-[0.5] ∼ SPR-[1], SPR-[0.25], and PtRu/C. Mass specific activities for methanol oxidation have been known to be influenced by CO stripping characteristics and mass specific active areas. Higher PtRu utilizations and an optimum surface structure with better CO tolerance are desirable for obtaining enhanced mass specific activity for methanol oxidation. In this experiment, it is possible that there were competitive contributions of PtRu utilization and CO stripping characteristics to the activity. A positive contribution of PtRu utilization and a negative contribution of CO stripping characteristics would compromise each other, resulting in the above activity order. The surface specific activities of the catalysts were calculated normalizing the oxidation current by electrochemical surface area, and the result is shown in Fig. 5 (b). PtRu/C shows the highest surface specific activity. In the SPR catalysts, the surface specific activity decreases with decreasing PtRu amount. This result is in accord with the result of CO stripping analysis. The strengthened Pt–CO and Ru–CO bonding on Au would cause lower surface specific activity. Although the surface specific activity of the PtRu overlayers on Au nanoparticles appeared to be stronger than that of PtRu/C, all PtRu overlayers on Au nanoparticles showed higher mass specific activity for methanol electro-oxidation, possibly due to high PtRu utilization.

4. Conclusion

The PtRu overlayers on Au nanoparticles were prepared with atomic-scale thicknesses, and their activity for methanol electro-oxidation was investigated. Based on the results of TEM, XRD and CV analysis, PtRu was found to be deposited on Au nanoparticles selectively. Peak and onset potentials from CO stripping analysis of the PtRu overlayers on Au nanoparticles appeared clearly different from each other. The peak and onset potentials shifted to higher potentials with decreasing PtRu amount, indicating stronger Pt–CO and Ru–CO bonding. PtRu utilization was enhanced up to 200% than that of PtRu/C with decreasing PtRu amount. The competitive contribution of CO stripping characteristics and PtRu utilization to methanol electro-oxidation led to SPR-[0.75] showing the highest mass specific activity. The strengthened Pt–CO and Ru–CO bonding would cause lower surface specific activity while the enhanced PtRu utilization would cause higher mass specific activity. In spite of the lower surface specific activities, all PtRu overlayers on Au nanoparticles showed higher mass specific activity for methanol electro-oxidation, possibly due to high PtRu utilization. Finding substrates which can improve intrinsic activity or reducing the particle size of substrates can be topics for future studies.

Acknowledgements

This work was supported by the Ministry of Commerce, Industry and Energy, the KOSEF through the Research Center for Energy Conversion & Storage and the Korea Research Foundation (Grant # KRF-2006-005-J04601).

References

[1] D. Zhao, B.-Q. Xu, Angew. Chem. Int. Ed. 45 (2006) 4955.
[2] D. Zhao, B.-Q. Xu, Phys. Chem. Chem. Phys. 8 (2006) 5106.
[3] I.-S. Park, K.-S. Lee, D.-S. Jung, H.-Y. Park, Y.-E. Sung, Electrochim. Acta 52 (2007) 5599.
[4] I.-S. Park, K.-S. Lee, J.-H. Choi, H.-Y. Park, Y.-E. Sung, J. Phys. Chem. C 111 (2007) 19126.
[5] M. Watanabe, S. Motoo, J. Electroanal. Chem. 60 (1975) 275.
[6] Y. Tong, H.S. Kim, P.K. Babu, P. Waszczuk, A. Wieckowski, E. Oldfield, J. Am. Chem. Soc. 124 (2002) 468.
[7] J.H. Zeng, J. Yang, J.Y. Lee, W.J. Zhou, J. Phys. Chem. B 110 (2006) 24606.
[8] B.C. Du, Y.Y. Tong, J. Phys. Chem. B 109 (2005) 17775.
[9] I.-S. Park, K.-S. Lee, Y.-H. Cho, H.-Y. Park, Y.-E. Sung, Catal. Today 132 (2008) 127.
[10] Y.D. Jin, Y. Shen, S.J. Dong, J. Phys. Chem. B 108 (2004) 8142.
[11] T.H. Hyeon, S.G. Han, Y.-E. Sung, K.-W. Park, Y.-W. Kim, Angew. Chem. Int. Ed. 43 (2003) 4252.
[12] S.-A. Lee, K.-W. Park, B.-K. Kwon, Y.-E. Sung, J. Ind. Eng. Chem. 9 (2003) 63.
[13] K.-W. Park, Y.-E. Sung, J. Ind. Eng. Chem. 12 (2006) 165.
[14] J.-H. Choi, K.-W. Park, B.-K. Kwon, Y.-E. Sung, J. Electrochem. Soc. 150 (2003) A973.
[15] I.-S. Park, B. Choi, D.-S. Jung, Y.-E. Sung, Electrochim. Acta 52 (2006) 1683.
[16] I.-S. Park, K.-W. Park, J.-H. Choi, C.R. Park, Y.-E. Sung, Carbon 45 (2007) 28.
[17] W. Alexander, J.E. Shackelford, CRC Materials and Engineering Handbook, 3rd ed., CRC, Boca Raton, 2001, p. 26.
[18] T.E. Lister, Y. Chu, W. Cullen, H. You, R.M. Yonco, J.F. Mitchell, Z.J. Nagy, Electroanal. Chem. 524–525 (2002) 201.
[19] J.X. Wang, N.S. Marinković, H. Zajonz, B.M. Pcko, R.R. Adžić, J. Phys. Chem. B 105 (2001) 2809.
[20] S. Štrbac, O.M. Magnussen, R.-J. Behm, J. Serb. Chem. Soc. 66 (2001) 119.
[21] A. Ruban, B. Hammer, P. Stoltze, H.L. Skriver, J.K. Norskov, J. Mol. Catal. A 115 (1997) 421.